J Mater Sci (2007) 42:7494–7501
DOI 10.1007/s10853-007-1588-8

Study on the reduction of highly porous TiO_2 precursors and thin TiO_2 layers by the FFC-Cambridge process

R. Lilia Centeno-Sánchez · Derek J. Fray · George Z. Chen

Received: 3 May 2006 / Accepted: 2 February 2007 / Published online: 18 May 2007
© Springer Science+Business Media, LLC 2007

Abstract Reduction of porous titanium oxide precursors by the FFC-Cambridge process is reported in this paper. Porous TiO_2 precursors were prepared by mixing the powder with different concentrations of graphite and polyethylene as fugitive agents and sintered at 1,073 K. The maximum porosity achieved before the mixture saturation was approximately 75%. After the electro-deoxidation by the FFC-Cambridge process, shrinkage of approximately 40% in volume and increase in porosity were observed, which might be due to atomic rearrangement, change of density and subsequent grain growth during reduction. The potential applied (below the decomposition potential of $CaCl_2$) had a direct effect on the minimum level of oxygen achieved, which was approximately 3,000 ppm for 48 h at 3.00 V and the same level at half the time (24 h) when increasing potential to 3.15 V. On the other hand, thin layers (300 μm thickness) screen-printed on titanium foils showed shorter reduction time than that observed for thicker porous pellets. This led to the conclusion that cathode geometry (porosity and thickness of the pellet) might have an effect on the rate of reduction by increasing the surface area available and improving the mass diffusion of oxygen ions.

R. L. Centeno-Sánchez · D. J. Fray (✉)
Department of Materials Science and Metallurgy,
University of Cambridge, Cambridge, UK
e-mail: djf25@cam.ac.uk

G. Z. Chen
School of Chemical, Environmental and Mining,
University of Nottingham, Nottingham, UK

Introduction

Titanium is an attractive engineering metal for many areas of application due to its unique set of properties: high strength, lightweight, good conductivity, biocompatibility with human tissue (when used as bone substitute) and resistance to corrosion. In particular, in areas such as medical and electrochemical technologies, titanium has attracted research efforts for the fabrication of parts with a porous microstructure. Porosity increases the titanium surface area, enhancing bone cell ingrowth in medical implants [1–3] as well as diminishing the bone-metal stiffness mismatch [1]. It also increases the overall electrode reaction rate in electrochemical systems [4–6]. Despite the advantages of this metal in the mentioned areas, the current process cost for its production is limiting and preventing the extensive exploitation of its unique properties. Therefore the present processing costs is cited as a critical factor that has driven research in the quest to find alternative means for its production [7, 8].

In the trend to develop a more efficient and less costly process for producing titanium, the FFC-Cambridge process (also known as direct electro-deoxidation) may be to be a viable route for reducing the cost to produce transition metals and their alloys by reducing metal oxides [9–11], which are less expensive and readily available. The reduction of solid TiO_2 by this novel route was first reported by Chen et al. [9]. In their study, the mechanism of the electro-deoxidation is described as the oxygen ionisation occurring at a less cathodic potential than the deposition of calcium, giving as a result the direct reduction of TiO_2 to Ti. In the process, the ionised oxygen is dissolved into the molten salt, discharging at and reacting with the graphite anode, leaving a major titanium phase at the cathode and producing CO and CO_2 gas at the anode, or oxygen gas if an inert anode is used. In this

process, the TiO_2 precursor is made the cathode, in order to remove the oxygen by electrolysis. The applied voltage must be greater than the potentials for the ionisation of oxygen but below the decomposition potential of the molten $CaCl_2$ salt [12, 13]. Table 1 shows the oxygen ionisation as the preferred reaction over the cathodic reaction of calcium deposition [14].

The general reaction at the cathode made of solid TiO_2, which gradually transforms to the metal as the reaction approaches completion, has been stated as [9]:

$$\mathrm{TiO}x + 2x\mathrm{e}^- = \mathrm{Ti} + x\mathrm{O}^{2-}. \quad (1)$$

Recent studies [15–18] have shown that the kinetic steps involved during the intermediate stages of this process are more complex. The presence of perovskites (calcium titanates) during early reduction stages and titanium sub-oxides prior to the completion of titanium de-oxidation have been observed, leading to the conclusion that the oxide goes through several oxidation states and phase transformations before being completely reduced to titanium. Schwandt and Fray [18] presented a more detailed study on the kinetic path followed during the electro-deoxidation process carried out under specific conditions, presenting the mechanisms of formation of calcium titanates and the gradual de-oxidation of titanium oxide until its completion, when a titanium–oxygen solid solution is formed. Chen and Fray [15], Jiang et al. [17] and Dring et al. [16] observed that cyclic voltammetric studies confirm that oxygen ionisation is the overall cathodic reaction, and it occurs at a more positive potential than the deposition of calcium.

On the other hand, at the anodic side of the cell, the following electrochemical reaction occurs as follows:

$$x\mathrm{O}^{2-} = (x/2)\mathrm{O}_2(\mathrm{g}) + 2x\mathrm{e}^-. \quad (2)$$

At the anode, graphite can react electrochemically with the dissolved oxygen ions producing CO_2 and CO gases in addition to O_2 (g), which are released:

$$x\mathrm{C} + x\mathrm{O}^{2-} = x\mathrm{CO} + x\mathrm{e}^- \quad (3)$$

$$x/2\mathrm{C} + x\mathrm{O}^{2-} = x/2\mathrm{CO}_2 + x\mathrm{e}^-. \quad (4)$$

The mechanisms of the FFC-Cambridge process are still being studied. Fray [14] observed the fact that although the initial and final states of the process are defined, the mechanism during the electro-deoxidation needs further studies. At present many efforts are being undertaken to understand in-depth the overall cell mechanisms in order to improve its performance.

Table 1 Electrode potentials

Electrode potentials in fused chlorides, calculated from thermodynamic data [E_{Na} = 0] at 973°K	
$O_2 + 4e^- = 2O^{2-}$	E° = 2.173
$TiO_2 + 4e^- = 2O^{2-} + Ti$	E° = 0.750
$Ca^{2+} + 2e^- = Ca$	E° = –0.060 V

The present research work is focused on reducing highly porous titanium oxide precursors and thin layers using the FFC-Cambridge process. It is also intended to study the effects of the cathode geometry on the reduction rate. This process presents a possible cost effective route to produce porous titanium preforms by direct reduction of TiO_2, this material being readily available. This process is carried out in the solid state and previous results have shown that oxide preforms can be reduced whilst preserving their approximate original shape.

Experimental procedure

A mixture consisting of TiO_2 (anatase, 99.9%), graphite, polyethylene and polystyrene as fugitive agents (pore former) 1,2-propanediol as binder, isopropyl alcohol as solvent and dispersant (Duramax D3021) was prepared to produce the porous precursors. The added dispersant was 0.3% of the mixture total volume. The total batch of titanium oxide powder used to prepare the precursors was first homogenised using a multiaxial blender. This step was performed to ensure the same particle size distribution (PSD) in all the precursors by minimising the difference in porosity among them. Also, thin layers produced by screen-printing the paste on 10×10 mm^2 titanium foil were reduced. Polystyrene with a monomodal distribution was synthesised in the laboratory to be used as a fugitive agent, however reductions were not carried out due to the toxicity and expenditure involved in preparing these mixtures.

The particle size distribution (PSD) for the TiO_2 powder and fugitive agent was measured using a Malvern Mastersizer 2000E. Results are shown in Fig. 1. Graphite presents a polydisperse particle size distribution while TiO_2 presents a bimodal distribution, which suggests the presence of agglomerates. Therefore an ultrasonic probe was used to prepare the mixture in order to break the agglomerates, avoiding later formation and ensuring a homogeneous porosity in all the prepared precursors.

The green precursors were prepared by casting the slip into 1 cm diameter polyethylene moulds and drying them in air. The approximate amount used to produce the pellet was 0.5 g. Table 2 shows the physical properties (data provided by chemicals vendor) and the experimental PSD data of the raw material used in the mixture preparation.

The green precursors were sintered at 1,073 K for 5 h using a furnace with extraction capabilities. At this stage the fugitive agent was burnt out completely from the pellet leaving behind a porous structure (porous precursor).

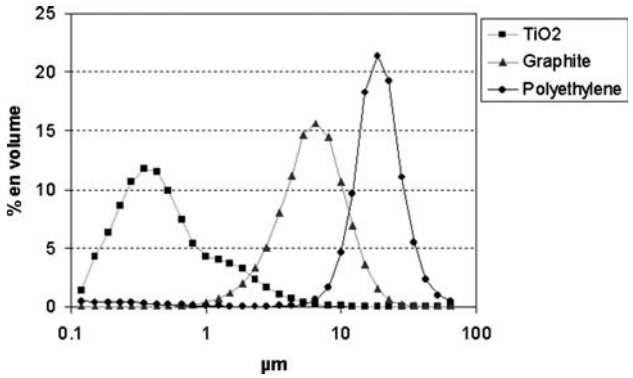

Fig. 1 Particle size distribution of TiO_2 and fugitive agents

Differential scanning calorimetry (DSC) and differential thermo-gravimetric (DTG) analysis were performed to determine the temperature at which graphite is leaving the structure as CO_2. The weight lost indicates the complete removal of graphite from the specimen. After sintering, the Archimedes method was used to calculate the porosity before and after reduction.

For electrolysis, the porous precursor was made the cathode and a high-density graphite rod supplied by Tokai Carbon UK, Ltd was used as the anode. The sintered porous TiO_2 and graphite were assembled to molybdenum rods. A schematic of the apparatus is shown in Fig. 2. The furnace temperature profile was obtained by measuring the temperature along the reactor using a thermocouple type K. The stainless steel crucible was positioned in the hottest zone (see Fig. 2b). Aldrich supplied the $CaCl_2{\cdot}2H_2O$, which was used to prepare the electrolyte. The salt was dehydrated in air at 473 K for 24 h and heated at 0.1 K/min to 623 K, holding this temperature for 8 h. Prior to the pellet reduction, a pre-electrolysis step was followed for approximately 2 h at 2.80 V in order to purify the electrolyte by removing the deleterious effects of moisture and by reducing contamination arising from metal impurities. Reduction of the pellet (containing 45% of graphite before sintering) was carried out at 1,173 K and 3.00 V for 12, 24, 48 and 72 h. The theoretical decomposition potential of the pure $CaCl_2$ salt at 1,173 K is estimated to be between 3.2655 V [12] and 3.213 V [19], much higher than that for the oxygen ionisation (refer to Table 1).

The reactor was filled with argon during the complete reduction time. A Wayne Kerr PSH3610 power supplier controlled the constant voltage applied. The time-current profiles for the samples reduction were recorded on a PC. After finishing the electrolysis the reduced sample was pulled up to the coolest area of the furnace (see Fig. 2b) and allowed it to cool down in an Ar atmosphere until the furnace temperature reached 973 K. The sample was then removed from the furnace, quenched and washed in cold water, followed by leaching in 1:1 acetic acid solution and 10% warm hydrochloric acid solution to remove residues of $CaCl_2$ remaining in the sample. After the cleaning process the samples were left to dry in a vacuum oven at 333 K for 12 h and sectioned to measure their porosity. The specimen microstructure was examined using a JEOL FEG–SEM (field emission gun–scanning electron microscope). Chemical analysis was performed using energy dispersive X-ray analysis (EDX). The samples were coated with platinum to avoid charging due to the probable presence of oxides in the sample. The content of oxygen in the reduced samples was determined by using an ELTRA ONH-2000 solid-state infrared absorption analyser.

Results and discussion

Figure 3 shows the SEM micrographs of the TiO_2-fugitive agents mixtures after carrying out the sintering process. Interconnected porosity is observed after the fugitive agent leaves the structure during sintering. Graphite and polyethylene show a polydisperse distribution. A third fugitive agent (polystyrene) synthesized in the laboratory shows a monomodal distribution. Reduction of precursors prepared with this material was not pursued due to the cost and toxicity of the chemicals involved on its preparation. However it can present an alternative to produce ordered oxide structures used in optical devices, photocatalysis, etc. [20, 21].

The porosity values obtained after the TiO_2–graphite and TiO_2–polystyrene mixtures were sintered to produce the porous precursors are shown in Fig. 4. The precursor shows no significant increase in porosity after 80% mass of graphite was added to the mixture. It can be observed that the saturation point is reached at approximately 45% mass of these fugitive agents in the mixture. Therefore, it was decided to select mixtures with this mass content to prepare the precursor for their later reduction by the FFC-Cambridge process. These mixtures do not involve toxic

Table 2 Physical properties of the raw materials used

Material	Melting point (°C)	Density (g/cm^3)	PSD range (µm)	PSD* D[v, 0.5] (µm)
Ti	1,668	4.506	–	–
TiO_2	1,835	3.9	0.1–10	0.48
Graphite KS-10	3,500	2.25	0.7–30	6.84
Polyethylene	144	0.940	10–100	46.42

*Particle size of the 50% bulk material

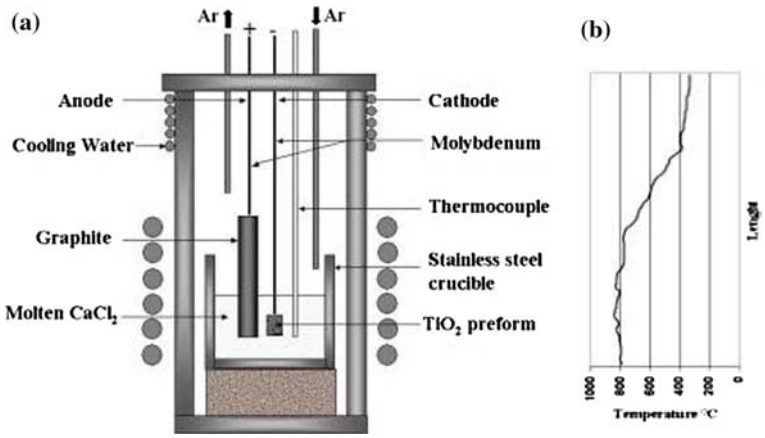

Fig. 2 Schematic of (**a**) FFC system used and (**b**) temperature profile inside the reactor

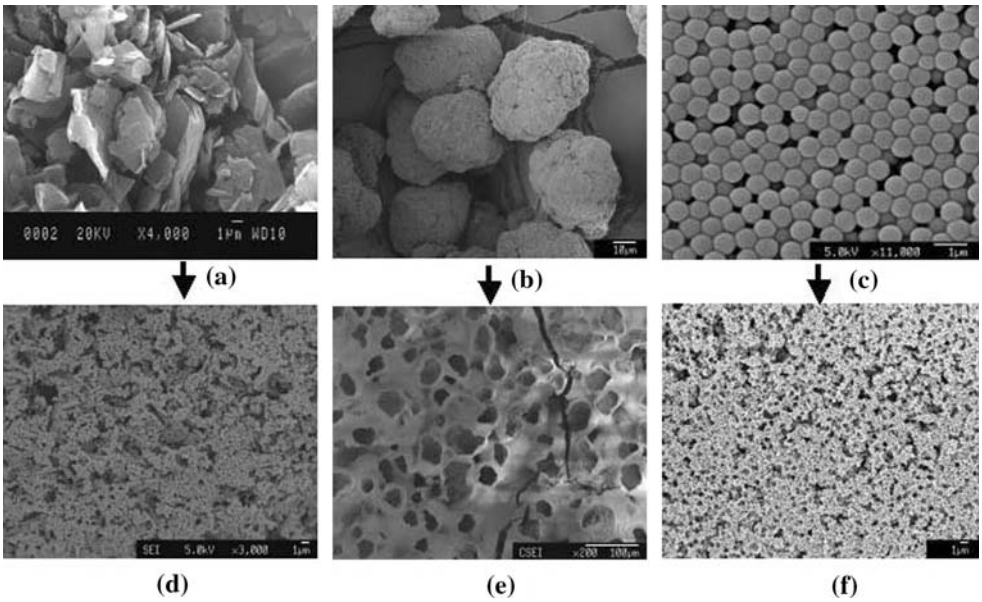

Fig. 3 Fugitive agents. (**a–c**) Graphite, polyethylene and polystyrene. (**d–f**) Respective porous TiO_2 microstructures using these fugitive agents

chemicals during preparation, they give a fairly good porosity (approximately 78–80%) and minimum amount of fugitive agent is used. Porosity for precursors prepared without fugitive agent had a similar value as that obtained when 30% of graphite was added to the mixture. This precursor showed a larger relative standard deviation (12%), in comparison to the other mixtures.

Figure 5 shows SEM micrographs of the structures after sintering the pellets containing a mixture of TiO_2 with varying graphite content. Interconnected porosity is observed after the fugitive agent leaves the structure during sintering. During this process graphite and oxygen reacts as follows:

$$C+O_2(g)\rightarrow CO_2(g)\ \Delta G^{\circ}=-94.603\text{Kcal},(973\text{K}-1{,}073\text{K}).$$

DSC measurements carried out in TiO_2/graphite mixtures showed that after combining with oxygen, graphite is completely removed leaving the TiO_2 structure as CO_2 (g) at approximately 1,009 K. Alternatively, for polyethylene, the fugitive decomposes at approximately 573 K.

After electro-deoxidation of the sintered precursor G45% (45% mass of graphite as a fugitive agent) a shrinkage effect of approximately 40% in volume was observed (see Fig. 6). Therefore after electro-deoxidation two possibilities were thought might have happened: the decrease of porosity due to the combined effect of shrinkage and atom rearrangement or the increase of porosity due solely to the atom re-arrangement occurring during reduction, which might increase the voids already produced by the use of the fugitive agent.

Figure 7 shows that the final effect is the increase rather than decrease in porosity for the porous precursor G45%. The graph shows a gradual increase of porosity with increasing deoxidation time. The maximum porosity achieved was at 48 h electro-deoxidation time. At this stage the porosity of the precursor increased about 12% with respect to its original value. At 72 h a decrease in

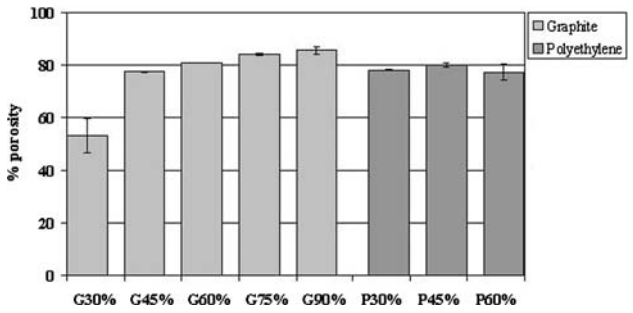

Fig. 4 Porosity achieved after sinterization of mixtures of TiO_2 with different content of graphite and polyethylene

porosity was observed, which might be due to the sample sintering. These observations suggest that the effects on the final porosity are directly related to atom re-arrangement, change of density and a sintering process.

FEG–SEM micrographs showing the microstructure of the reduced G45% pellets are presented in Fig. 8. It should be noted that after the oxygen has left the structure, an increase in the grain size (with respect to the original structure of the TiO_2 pellet) is observed due to atom rearrangement during reduction. The pore sizes increased approximately 5–10 times their original size, which explains the increase in porosity despite the shrinkage effect. Interconnected porosity was observed after reduction in all samples.

Figure 9 shows the SEM–EDX elemental analysis confirming the presence of a major phase of titanium in the reduced pellets. The analysis indicates the presence of a small amount of oxygen for samples reduced at 24 and 48 h using 3.00 V (refer to Fig. 12). In some specimens, a very weak signal of iron was detected by this technique. This element might be a result of mechanical cross-contamination during washing due to the stainless steel mesh used as sample holder and being in contact with the sample, which becomes brittle after the reduction process. Other possible source might be the stainless steel crucible.

Figure 10 shows a thin film of TiO_2 (approximately 300–400 μm thickness) screen-printed on titanium foil. Figure 10b shows the metal–oxide interface, which promotes adhesion. These precursors were reduced under the same conditions than thicker pellets, as previously described.

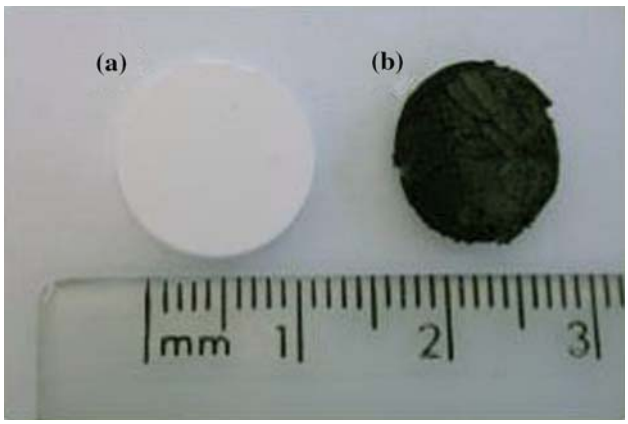

Fig. 6 Precursor (**a**) after sintering and (**b**) after electro-deoxidation

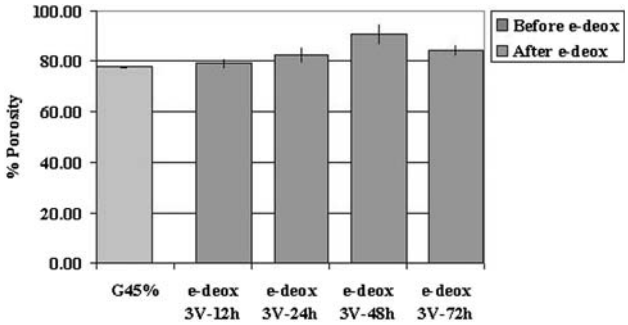

Fig. 7 Porosity after different reduction times for precursors containing 45% mass of graphite before sinterization

Figure 11 presents the thin oxide layer after reduction. EDX analysis clearly shows the presence of titanium. After reduction partial delamination was observed, which might have occurred during reduction.

Figure 12 shows the oxygen content analysis of the G45% pellets reduced at 3.00 V and the thin layer specimen. The graph for thicker pellets (3 mm) indicates that the oxygen content is decreasing while the reduction time is increasing. The minimum amount of oxygen achieved was approximately 3,000–4,000 ppm. It was also observed that increasing the voltage to 3.15 V reduces the electro-deoxidation time approximately by half. A similar value was observed for precursors prepared with polyethylene,

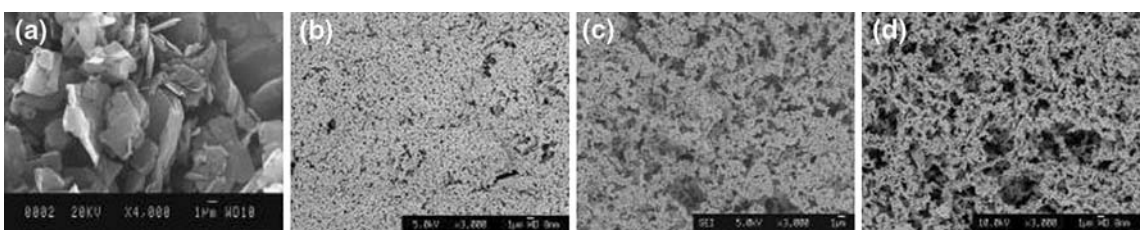

Fig. 5 Microstructures at 3,000× (**a**) graphite, (**b**) mixture G30%, (**c**) mixture G60%, (**d**) mixture G90%. The porous TiO_2 microstructures at 3,000×

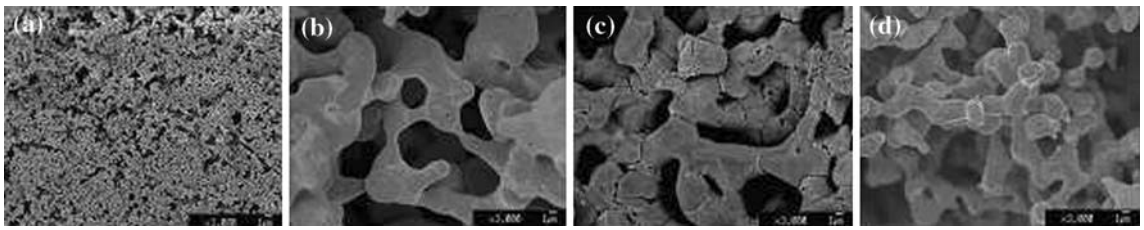

Fig. 8 SEM micrographs from pellets G45% (**a**) after sintering, (**b**) e-deox. 24 h, (**c**) e-deox. 48 h and (**d**) e-deox. 72 h

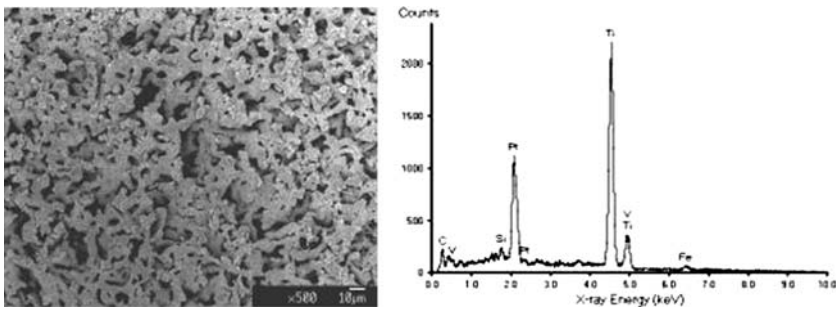

Fig. 9 EDX analysis from an electro-deoxidised sample at 24 h 3 V

P45%, showing the same porosity. These results suggest that the voltage applied has a direct effect on the electro-deoxidation rate. On the other hand the time of reduction was much lower for thin layers (300–400 μm) than that observed during reduction of much thicker pellets. Figure 12 shows that after 6 h of reduction, the thin layer contains much less oxygen than that observed after 12 h in a thicker pellet. This suggests that besides porosity, thickness is another parameter that also affects the rate of reduction.

Regardless the type of fugitive agent, when the same porosity is achieved the minimum amount of oxygen achieved was approximately 3,000–4,000 ppm, whereas pellets not containing fugitive agent and porosities below 50% showed a larger amount of oxygen, at the same reduction time. See Fig. 13.

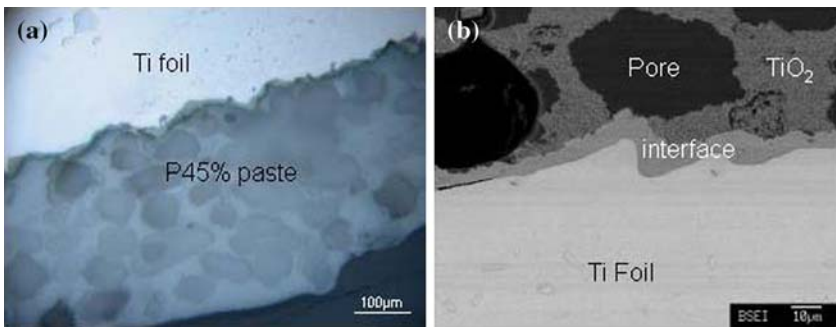

Fig. 10 TiO_2 thin films. (**a**) TiO_2 thickness and (**b**) metal–oxide interface

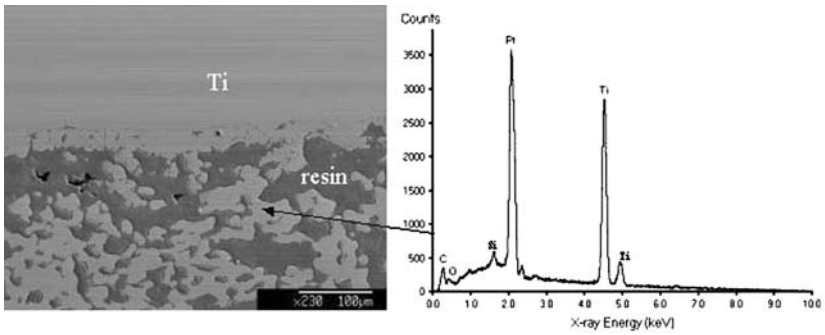

Fig. 11 Thin TiO_2 layer after reduction

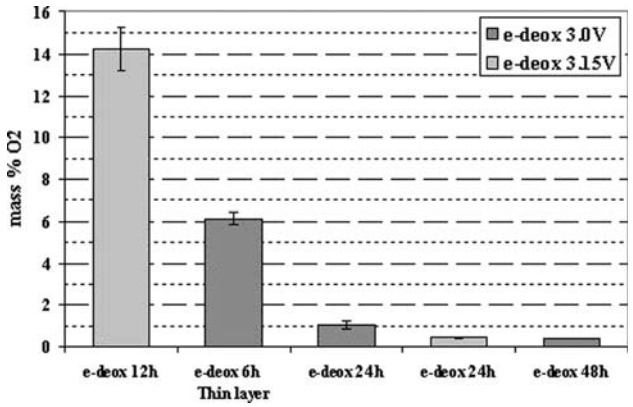

Fig. 12 O_2 % mass at different reduction times for G45% pellets

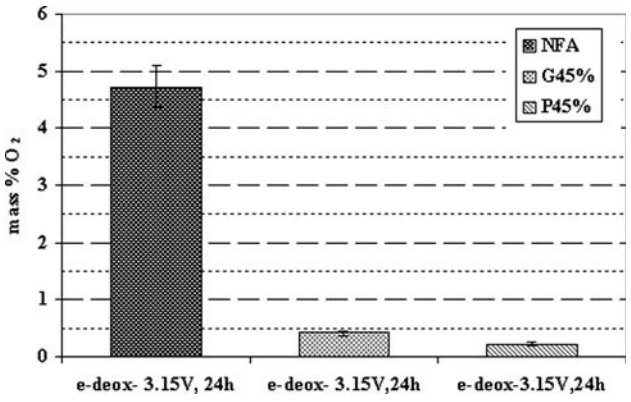

Fig. 13 Oxygen content for precursors prepared without fugitive agent and with fugitive agent

Figure 14 shows the XRD patterns from titanium oxide (anatase) as received, a specimen produced by the Kroll process and the reduced pellets at 3.00 and 3.15 V, respectively, for 24 h. In these pellets a major phase of titanium is present. In both cases titanium is present in its two crystalline structures: cubic and hexagonal. In comparison, the same phases for titanium are also found in the sample reduced by the Kroll process, although in different proportion, as is clearly observed by the intensity ratios shown in the diffraction patterns. Hongquiite, a minor phase of titanium oxide is also identified. The presence of this oxide phase suggests that titanium goes through different oxidation states before its complete reduction, whereas the weak signal of titanium carbide suggests deposited carbon during the reduction process. Although this compound is rarely found at the end of reduction, general interaction with carbon within the cell environment requires further studies. The square scale used to present the XRD patterns enhances the presence of low concentration peaks therefore it is important to bear in mind that while their presence is noticeable in this scale their concentration is very low in a linear scale, which is used for quantification purposes. The Relative Intensity Ratio (RIR) estimates the approximate concentration of the oxide phase present below 0.3% by the XRD technique.

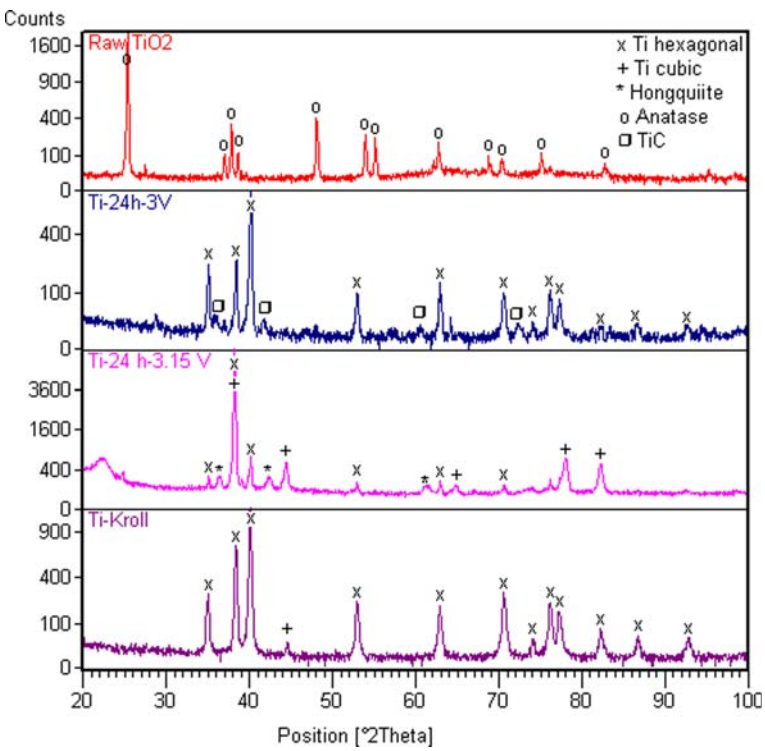

Fig. 14 XRD patterns of the raw material and reduced samples

The presence of cubic titanium might be due to some retained cubic phase or transformed beta formed during initial cooling to room temperature, when the sample is brought up to the coolest zone of the reactor (as shown in Fig. 2b) to be later quenched in water. In titanium metallurgy the common present phases are classified into three categories: α (hexagonal), $\alpha + \beta$ and β (cubic), which describe the origin of the microstructure in terms of the basic crystal structure favoured by an alloy composition. The basic structure α changes to β and back again when heated and cooled down. However the α–β alloy consists of α and retained or transformed β [22]. These alloys can be strengthened at a temperature in the field of the two-phase α–β and followed by quenching in water. As a result of quenching, the β phase present at the water-quenching temperature may be retained or may be partially transformed during cooling by either martensitic transformation or nucleation and growth, which explains the presence of low concentration of cubic titanium in the sample.

Conclusions

The results have shown that porous oxide preforms can be reduced while preserving their approximate shape with interconnected or open porosity. Precursors with porosity >75% were produced either by using graphite or polyethylene as fugitive agent. The volume shrinkage observed might be due to atomic rearrangement and change of density due to the phase transformations occurred throughout the reduction process. The minimum oxygen content achieved by this process in highly porous precursors was approximately 0.3% mass after 48 h reduction time at 3.00 V and half the time (24 h) when increasing the potential to 3.15 V. This shows the effect of potential on the rate of reduction. Furthermore, cathode geometry (porosity and thickness) also has a direct effect on the rate of reduction. Both porosity and thickness are related to the available surface area in contact with the electrolyte, and diffusion distance, which when decreased might also improve mass diffusion of the oxygen ions.

The scope of this paper is to present the effect of porosity in the rate of reduction, as well as preparing porous titanium structures. The kinetics and mechanisms of reaction are to be discussed in a following publication.

Acknowledgments The authors would like to acknowledge to Regenesys Technologies Ltd, UK and the *Consejo Nacional de Ciencia y Tecnología* (CONACYT), Mexico for financial support of this research.

References

1. Ik-Hyun O, Naoyuki N, Shuji H (2002) Mater Trans 43:443
2. Thelen S, Barthelat F, Brinson LC (2004) J Biomed Mater Res A 69A:601
3. Li HL, Oppenheimer SM, Stupp SI, Dunand DC, Brinson LC (2004) Mater Trans 45:1124
4. Larminie J, Dicks A (2000) Fuel cells systems explained. John Wiley & Sons, Inc., New York, p 5
5. Lipp L, Pletcher D (1997) Electrochim Acta 42:1091
6. Lindbergh G, Olivry M, Sparr M (2001) J Electrochem Soc 149:A411
7. Froes FH (1998) JOM 50:15
8. Hartman AD, Gerdemann SJ, Hansen JS (1998) JOM 50:16
9. Chen GZ, Fray DJ, Farthing TW (2000) Nature 407:361
10. Yan XY, Fray DJ (2002) Metall Mater Trans B 33B:685
11. Yan XY, Fray DJ (2003) J Mater Res 18:346
12. Delimarskii IK (1975) Electrochemistry of fused salts. Sigma Press Publishers, Washington, DC
13. Ono K, Suzuki RO (2002) JOM 54:59
14. Fray DJ (2002) Can Metall Q 41:433
15. Chen GZ, Fray DJ (2002) J Electrochem Soc 149:E455
16. Dring K, Dashwood R, Inman D (2005) J Electrochem Soc 152:E104
17. Jiang K et al (2006) Angew Chem Int Ed 45:428
18. Schwandt C, Fray DJ (2005) Electrochim Acta 51:66
19. Suzuki RO, Teranuma K, Ono K (2003) Metall Mater Trans B 34B:287
20. Meng QB, Go ZZ, Sato O (2000) Appl Phys Lett 77:4313
21. Brian BT, Blanford CF, Stein A (1998) Science 281:538
22. Donachie MJ Jr (1988) Titanium: a technical guide. ASM International, USA, p 6